2014 Spring

"Advanced Physical Metallurgy"

- Bulk Metallic Glasses -

05.27.2014

Eun Soo Park

Office: 33-313
Telephone: 880-7221
Email: espark@snu.ac.kr
Office hours: by appointment

5.7. Annealing of Bulk Metallic Glasses: SR → SCLR (& PS) → Crystallization

Figure 5.11 Different pathways for a metallic glass to crystallize into the equilibrium phases

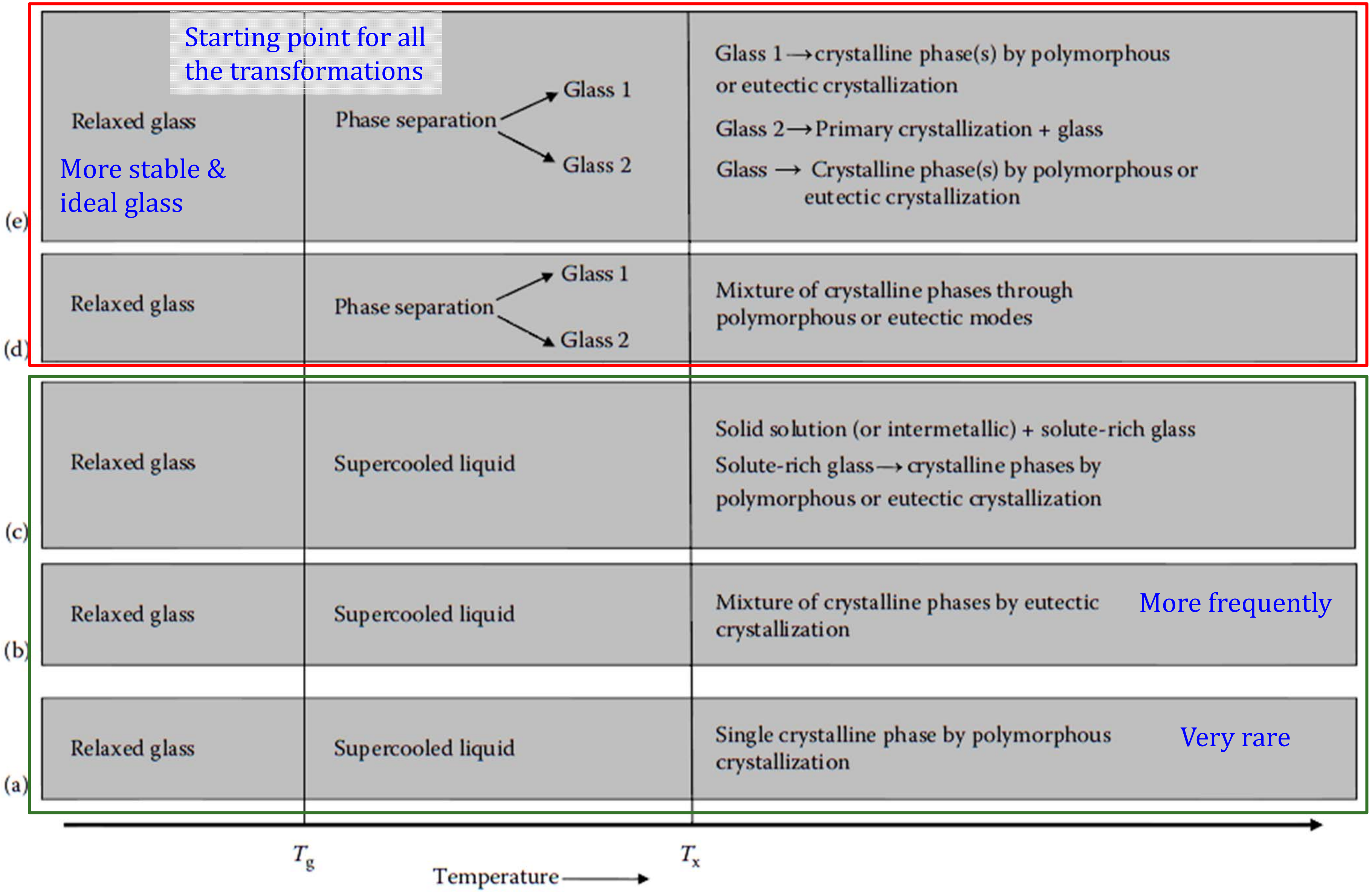

* Measurement of structural relaxation in metallic glasses:

- Electrical resistivity measurements (CSRO < TSRO) and DSC (most popular technique)
- Mossbauer spectroscopy (determine the atomic environments)
- Hardness measurement (increased)
- Diffraction techniques (X-ray, neutron, and electron scattering methods)

(sharpening of the PDF peaks, without shifting their position)

→ The first stage of relaxation was suggested to be related to the elimination of short and long inter-atomic distances and the second stage to the local chemical reordering in the glassy phase (phase separation and nano-crystallization after annealing at higher temp.

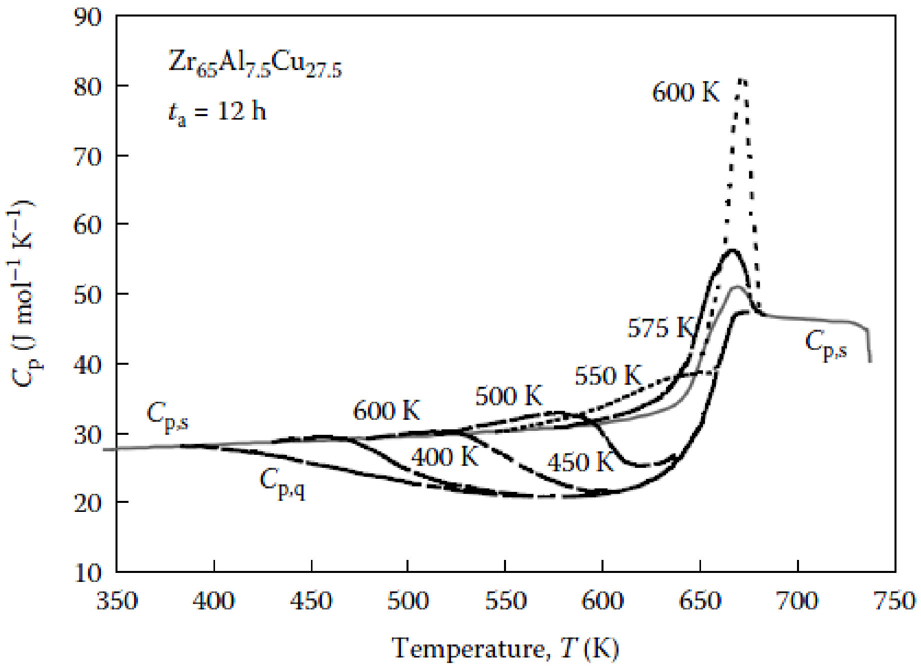

FIGURE 5.12
The variation of specific heat, C_p with annealing temperature, T_a for a glassy $Zr_{65}Al_{7.5}Cu_{27.5}$BMG alloy annealed for 12 h at different temperatures from 400 to 620 K. The solid line represents the variation of C_p for the reference sample annealed for 12 h at 690 K. (Reprinted from Inoue, A. et al., *J. Non-Cryst. Solids*, 150, 396, 1992. With permission.)

→ dependent on thermal history, excess endothermic peak (recoverable), exothermic broad peak (irrecoverable)

Dynamic mechanical relaxations in typical glasses

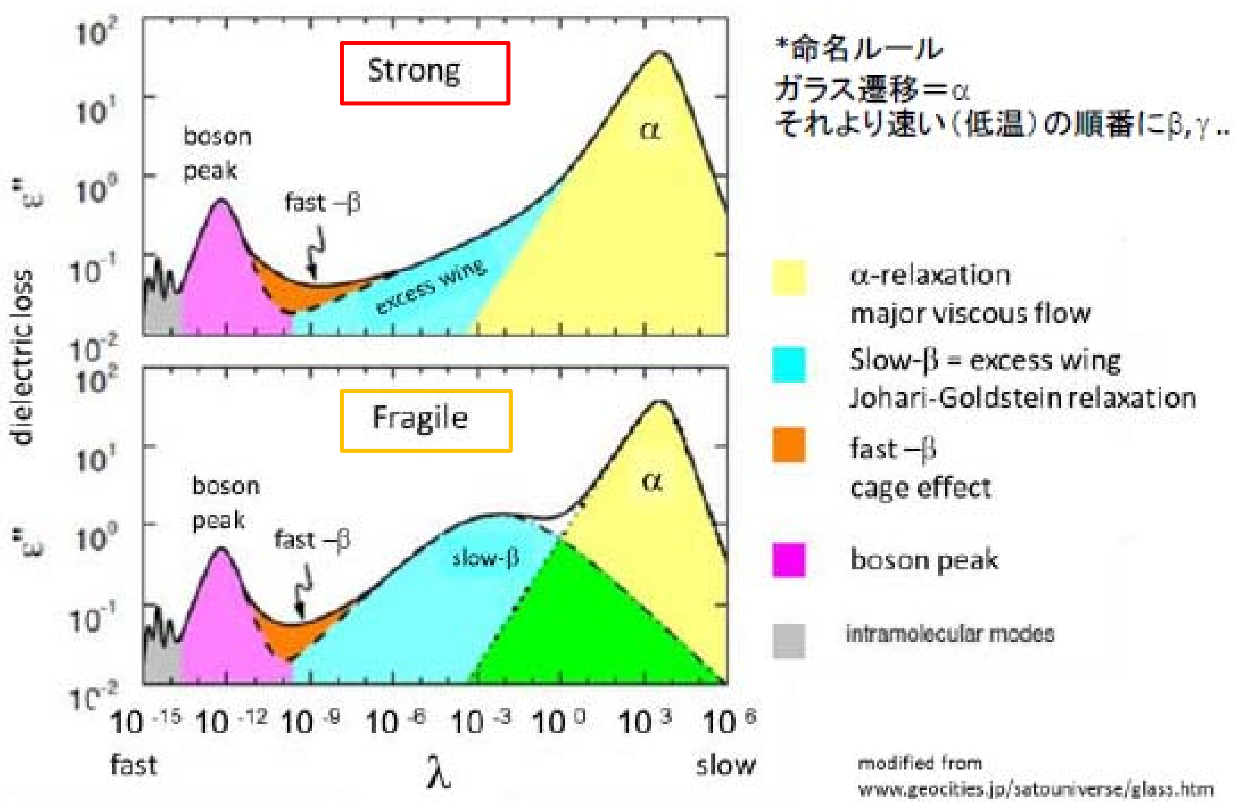

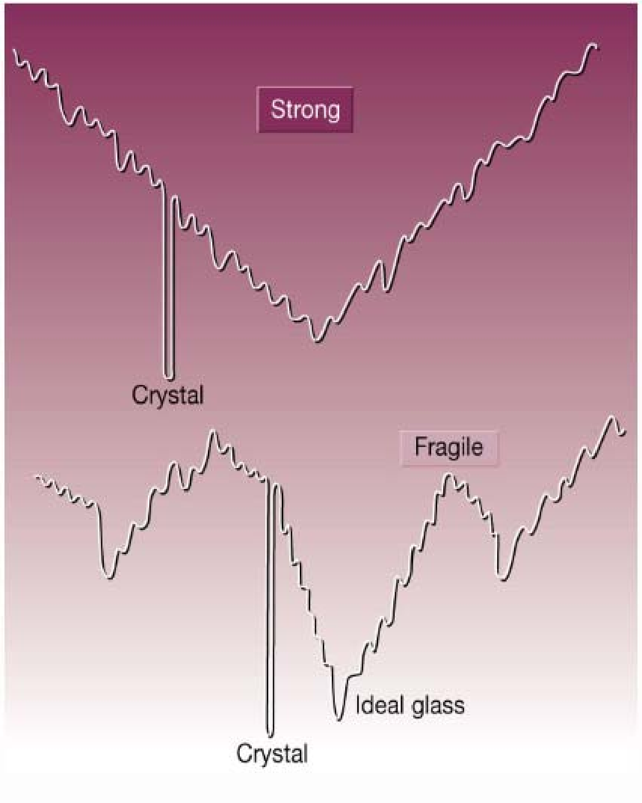

Schematic representation of the energy landscapes of strong and fragile substances.

Strong: small deviation of activation E
between α relaxation and β relaxation

Fragile: large deviation of activation E
between α relaxation and β relaxation

structural inhomogeneity correlating to slow-β

- Weakly & strongly bonded regions

  <u>Ichitsubo et al</u>, PRL95, 245501 (2005)
  & JNCS357, 494 (2011)

  The size ξ of SBR
  ~ 4 nm in Pd-Ni-Cu-P
  ~1.5 nm in Zr-Al-Ni-Cu

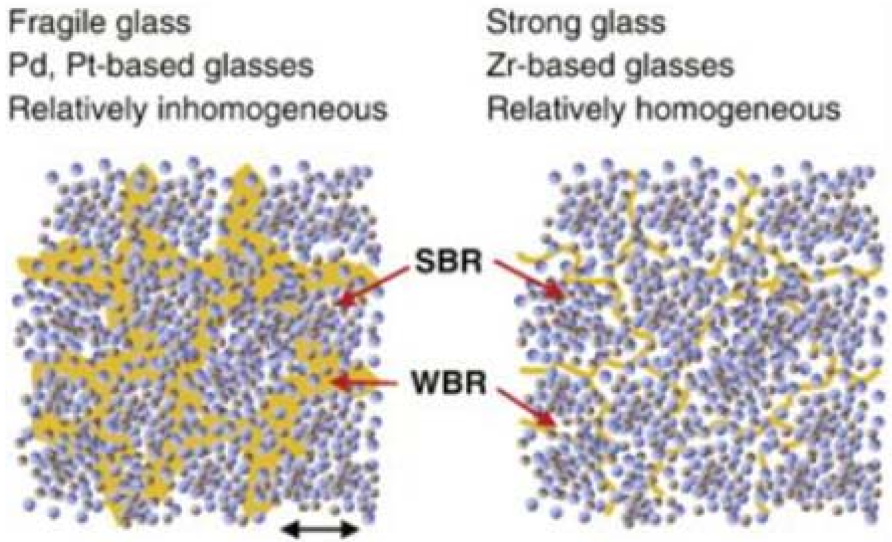

WBR, JG-relaxation & STZ

<u>Wang et al</u>, PRB75, 174201 (2007)
Local motion in the loser region below Tg
Q_β~ 28.4RTg (alloy dependence)

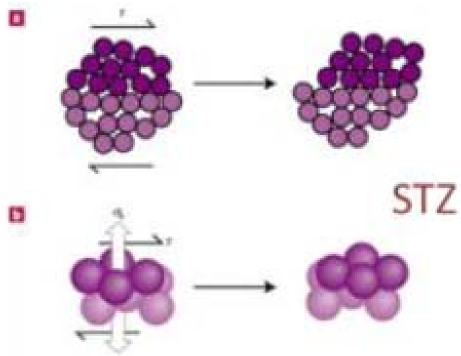

Annealing of Bulk Metallic Glasses: SR → SCLR (& PS) → Crystallization

5.7.2 Glass Transition: abrupt variation of C_p

Acta Materialia 59 (2011)

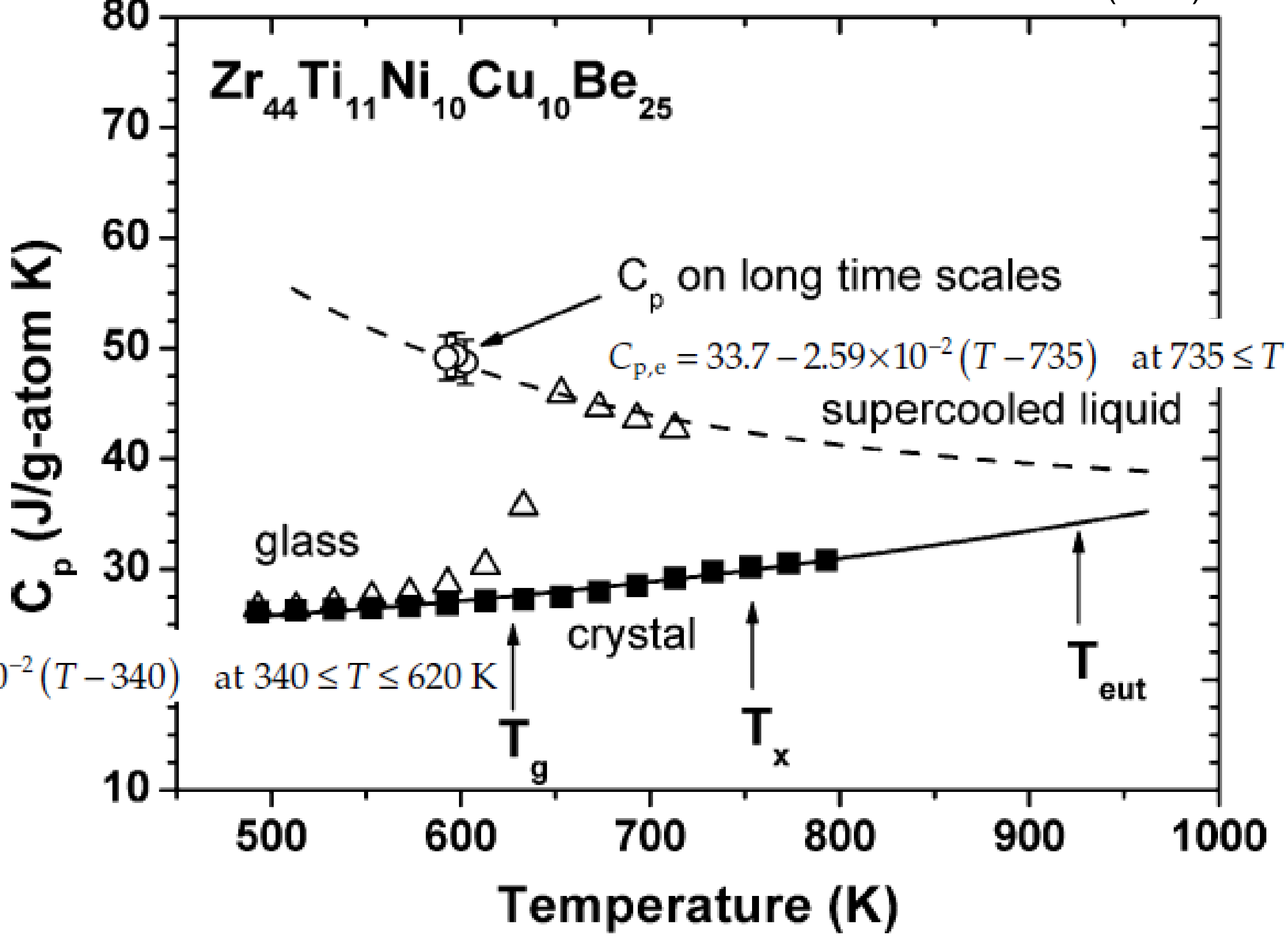

$C_{p,e} = 33.7 - 2.59\times10^{-2}(T - 735)$ at $735 \le T \le 760$ K

$C_{p,v} = 23.9 + 1.29\times10^{-2}(T - 340)$ at $340 \le T \le 620$ K

Annealing of Bulk Metallic Glasses: SR → SCLR (& PS) → Crystallization

5.7.3 Phase separation

* Miscibility gaps in phase separating system

- Stable immiscibility

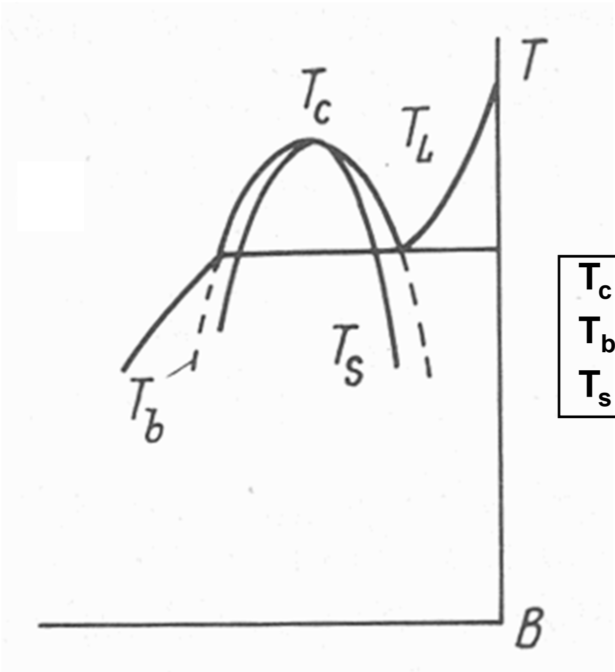

immiscibility above the liquidus

⇒ decomposition into stable liquid

T_c : critical temperature
T_b : binodal curve
T_s : spinodal curve

- Metastable immiscibility

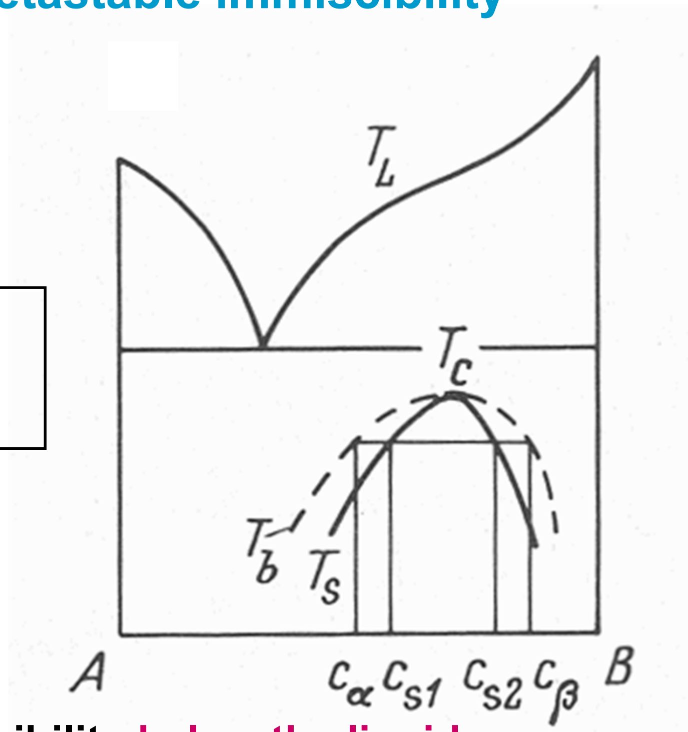

immiscibility below the liquidus

⇒ decomposition into metastable liquid

"Phase separation in glass" ed. by Mazurin and Porai-Koshits (1984)

(a) Positive heat of mixing relation among constituent elements

- **Alloy design considering heat of mixing relation among constituent elements**

$\Delta H_{mix} \gg 0$ between A & B

⬇

creates (meta)stable miscibility gap in limited composition range

⬇

Phase separation to A-rich & B-rich phase

- **Different two-phase structure by initial composition before phase separation**

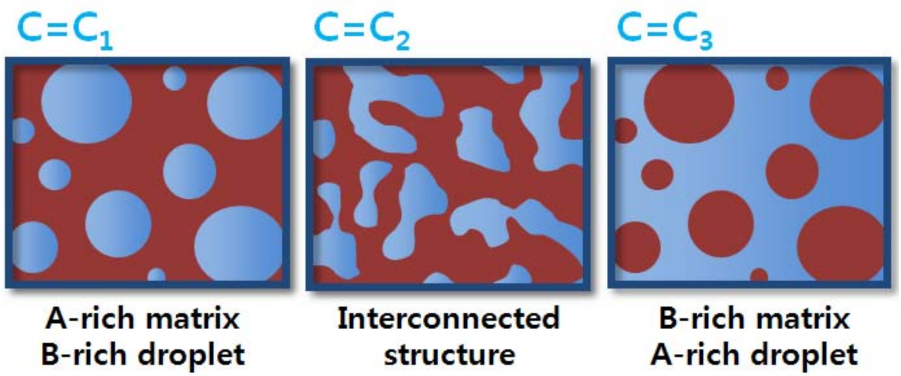

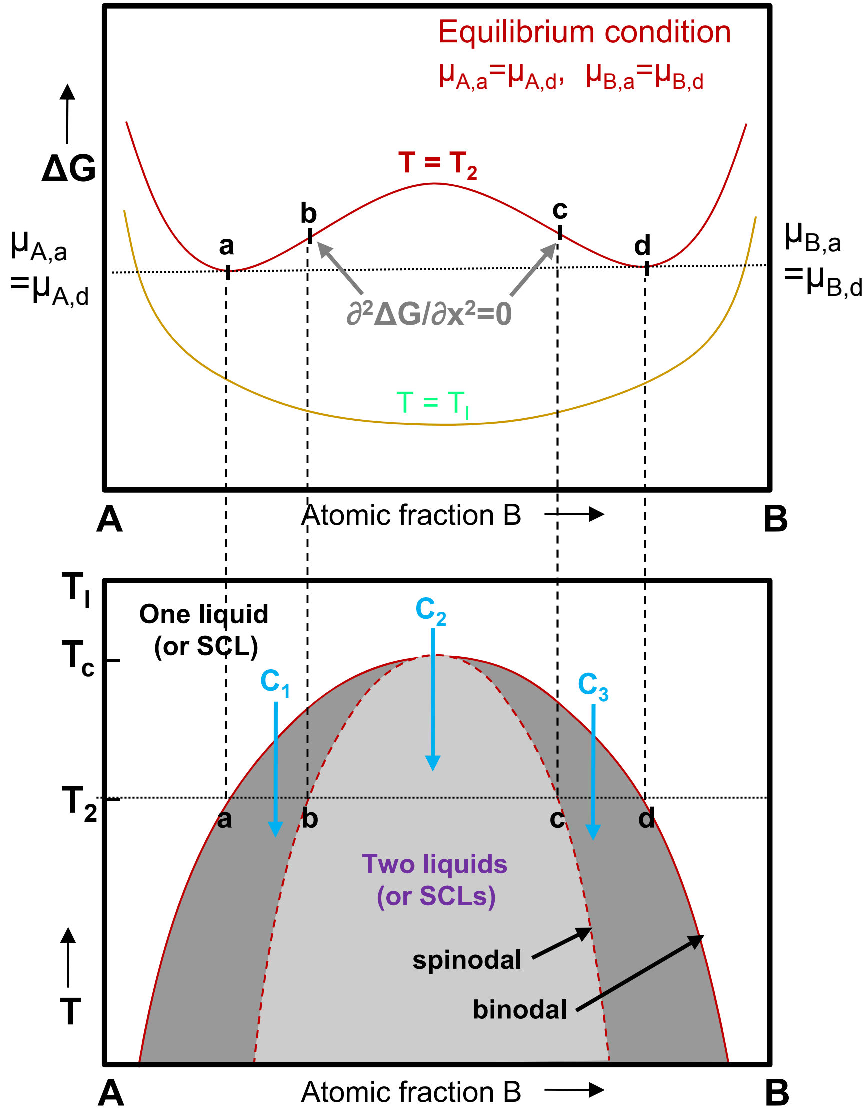

Nucleation and growth ↔ Spinodal decomposition without any barrier to the nucleation process

5.5.5 Spinodal Decomposition

Spinodal mode of transformation has no barrier to nucleation

: describing the transformation of a system of two or more components in a metastable phase into two stable phases

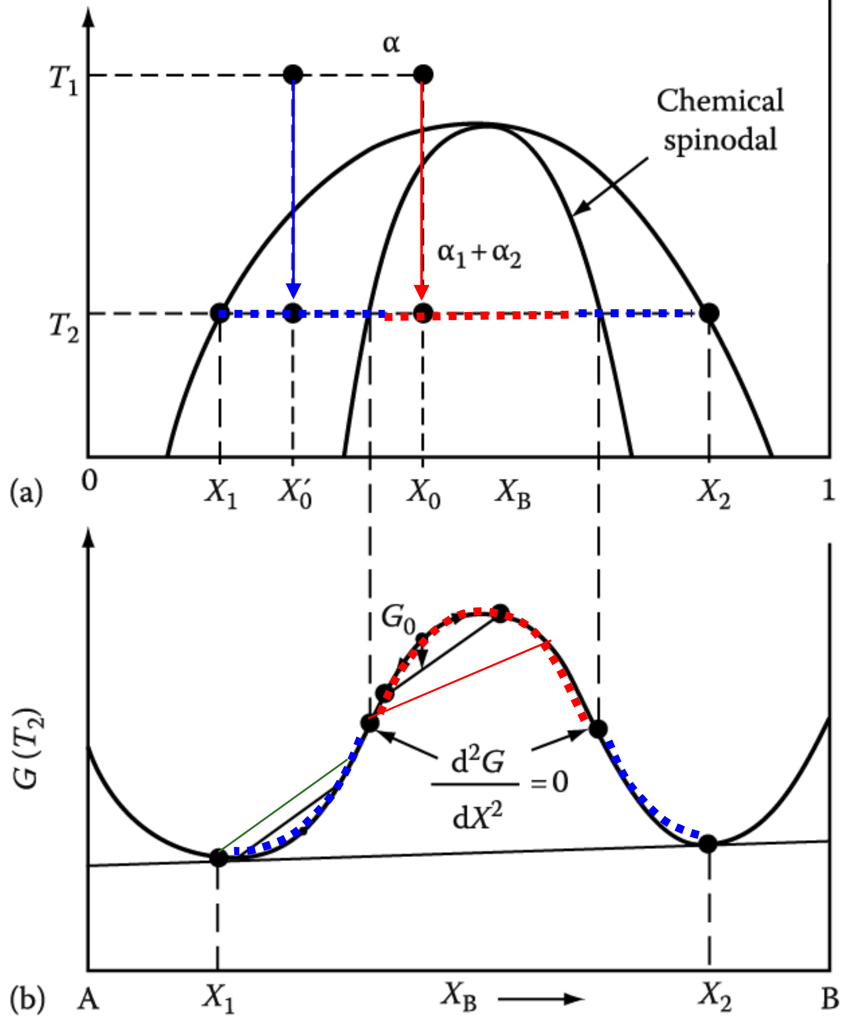

Fig. 5.38 Alloys between the spinodal points are unstable and can decompose into two coherent phasees α_1 and α_2 without overcoming an activation energy barrier. Alloys between the coherent miscibility gaps and the spinodal are metastable and can decompose only after nucleation of the other phase.

How does it differ between inside and outside the inflection point of Gibbs free energy curve?

1) Within the spinodal $$\frac{d^2G}{dX^2} < 0$$

: phase separation by small fluctuations in composition/ **"up-hill diffusion"**

2) If the alloy lies outside the spinodal, small variation in composition leads to an increase in free energy and the alloy is therefore metastable.

The free energy can only be decreased if nuclei are formed with a composition very different from the matrix.

→ nucleation and growth

: "down-hill diffusion"

a) Composition fluctuations within the spinodal

b) Normal down-hill diffusion outside the spinodal

up-hill diffusion

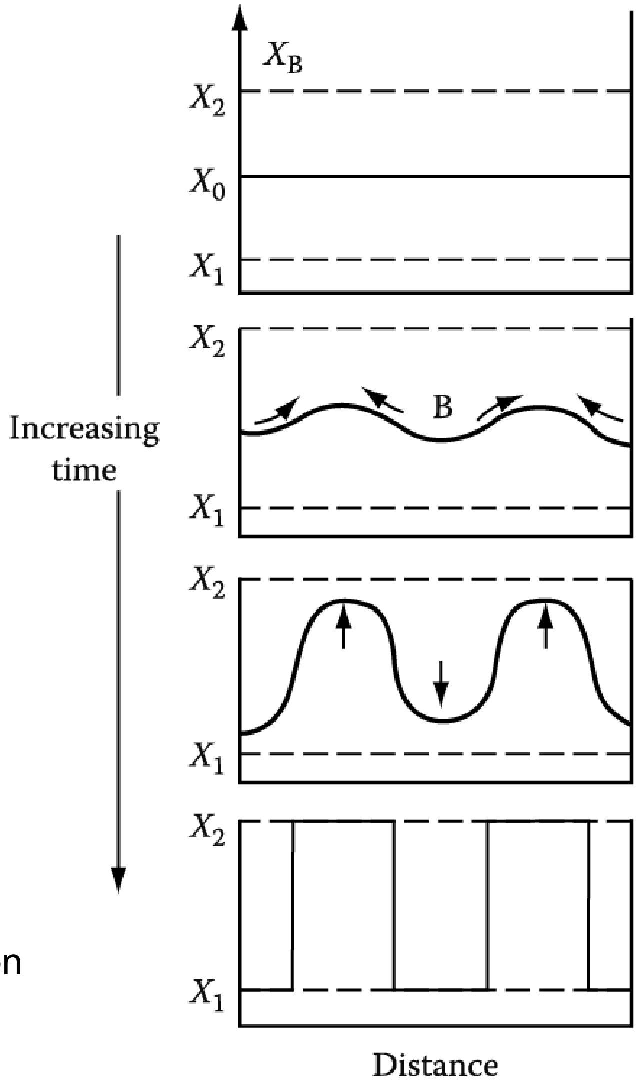

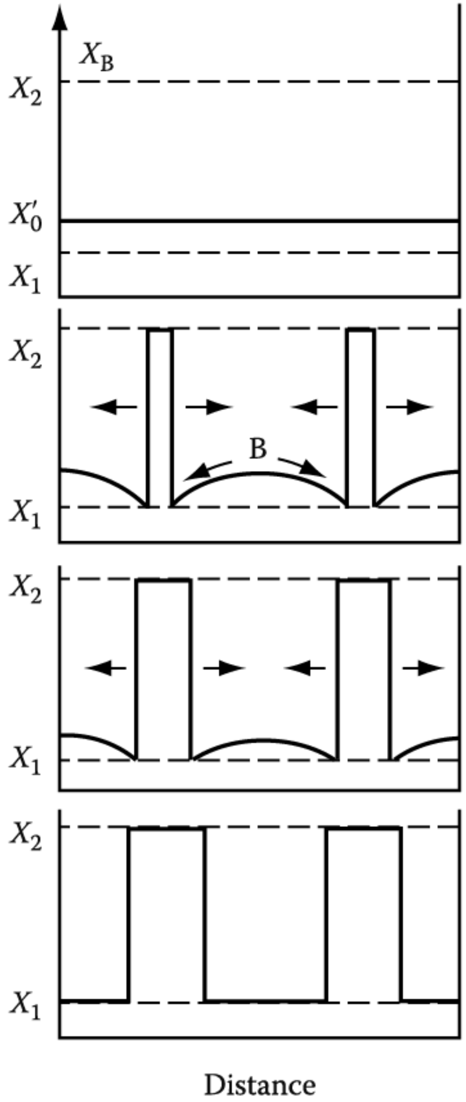

down-hill diffusion

interdiffusion coefficient
D<0

Fig. 5.39 & 5.40 schematic composition profiles at increasing times in (a) an alloy quenched into the spinodal region (X_0 in Figure 5.38) and (b) an alloy outside the spinodal points (X_0' in Figure 5.38)

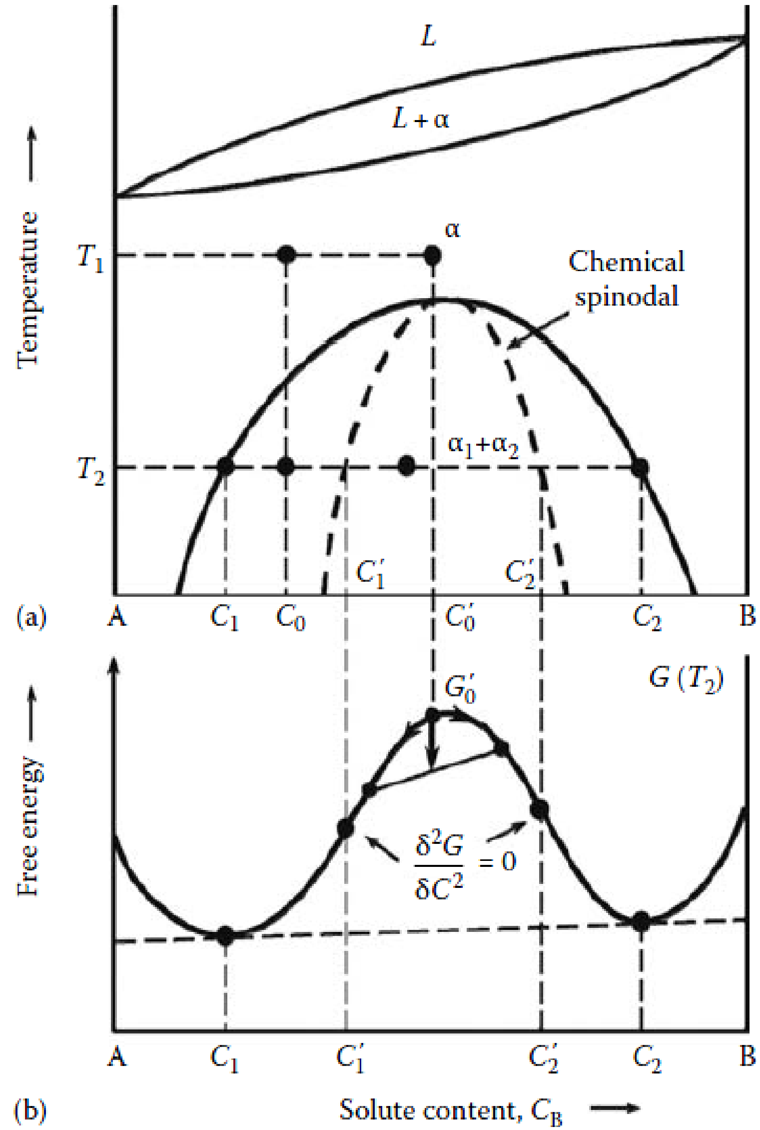

FIGURE 5.14
(a) Typical phase diagram showing a miscibility gap in the solid state. (b) The corresponding free-energy vs. composition diagram featuring two minima. Phase separation is possible in such an alloy system either by a nucleation and growth process or by a spinodal decomposition process.

TABLE 5.5

Alloy Systems Showing Phase Separation in the Glassy State

Alloy Composition	Synthesis Method	Characterization Method(s)	Compositions of the Two Glassy Phases	Comments	References
$Ag_{20}Cu_{48}Zr_{32}$	Melt spinning	TEM			[93]
$Cu_{43}Zr_{43}Al_7Ag_7$	Cu-mold casting	TEM and 3DAP	$Cu_{40.7}Zr_{46.8}Al_{8.0}Ag_{4.5}$ and $Cu_{36.8}Zr_{43.5}Al_{7.0}Ag_{12.7}$	Phase separation due to unusually high plastic strain	[94]
$Cu_{46}Zr_{22}Y_{25}Al_7$	Melt spinning	DSC and TEM	$Cu_{35.7}Zr_{12.8}Y_{44.3}Al_{7.2}$ and $Cu_{53.4}Zr_{31.8}Y_{8.3}Al_{6.5}$		[95]
$La_{27.5}Zr_{27.5}Al_{25}Cu_{10}Ni_{10}$	Melt spinning	SEM and TEM	$La_{5.0}Zr_{51.4}Cu_{5.4}Ni_{13.2}Al_{25}$ and $La_{43.4}Zr_{10.9}Cu_{14.4}Ni_{8.2}Al_{22.1}$		[96]
$Nd_{60-x}Zr_xAl_{10}Co_{30}$ ($6 \leq x \leq 40$)	Melt spinning	DSC and TEM			[97]
$Ni_{70}Nb_{15}Y_{15}$	Melt spinning	DSC, TEM, and SAXS			[98]
$Ni_{66}Nb_{17}Y_{17}$	Melt spinning	DSC, TEM, and SAXS			[98]
$Ni_{58.5}Nb_{20.25}Y_{21.25}$	Melt spinning	DSC, SEM, TEM, and SAXS	$Ni_{59}Nb_{16}Y_{25}$ and $Ni_{57}Nb_{28}Y_{15}$ by SEM and $Ni_{53}Nb_{42}Y_5$ and $Ni_{60}Nb_{10}Y_{30}$ by TEM	No two T_gs were observed	[98,99]
$Ni_{54}Nb_{23}Y_{23}$	Melt spinning	DSC, TEM, and SAXS	$Ni_{50}Nb_{44}Y_6$ and $Ni_{58}Nb_7Y_{35}$		[98]
$Ni_{61}Zr_{28-x}Nb_7Al_4Ta_x$ ($x = 0, 2, 4, 6, 8$)	Melt spinning			No evidence of phase separation	[100]
$Pd_{80}Au_{3.5}Si_{16.5}$	Roller quenching	DSC and SAXS		Apparent phase separation	[31]
$Pd_{78}Au_6Si_{16}$	Splat cooling	DSC and TEM	Segregation into (Pd–Au)-rich and Si-rich glassy phases	No clear identification of the phases	[30]
$Pd_{40.5}Ni_{40.5}P_{19}$	Centrifugal spinning	DSC		Two T_gs were observed only after the original glassy sample was heated beyond the first exothermic peak, then cooled quickly and reheated	[34]

TABLE 5.5 (continued)

Alloy Systems Showing Phase Separation in the Glassy State

Alloy Composition	Synthesis Method	Characterization Method(s)	Compositions of the Two Glassy Phases	Comments	References
$Pd_{80}Si_{20}$	Splat cooling	DSC and TEM	Pd-rich particles embedded in a Si-rich matrix	No clear identification of the phases	[30]
$Ti_{28}Y_{28}Al_{24}Co_{20}$	Melt spinning	XRD and TEM	$Y_{40.4}Ti_{14.7}Al_{21.9}Co_{23}$ and $Ti_{45.6}Y_{11.6}Al_{26.7}Co_{16.1}$	No clear T_g in DSC	[101]
$Ti_{56-x}Y_xAl_{22}Co_{22}$ ($x = 11$, 20, or 28)	Melt spinning	TEM	$Y_{44.5}Ti_{8.8}Al_{36.9}Co_{9.8}$ and $Ti_{47.2}Y_{2.1}Al_{19.9}Co_{30.8}$ These compositions depend on the initial composition of the alloy.		[102]
$Zr_{63.8}Ni_{16.2}Cu_{15}Al_5$	Cu-mold casting		$Zr_{68.5}Cu_{8.1}Ni_{21.3}Al_{2.1}$ and $Zr_{62.4}Cu_{16.7}Ni_{14.6}Al_{6.3}$	Noted 30% plastic strain during compression at room temperature	[103]
$Zr_{36}Ti_{24}Be_{40}$	Melt spinning	DSC and TEM		Two T_gs were reported. Nagahama et al. [104] concluded that this alloy crystallized in a eutectic mode and that there was no phase separation	[89]
$Zr_{52.5}Ti_5Cu_{17.9}Ni_{14.6}Al_{10}$ (Vit 105)	Cu-mold casting and Melt spinning	SANS and TEM		Phase separation? Kajiwara et al. [106] suggested primary crystallization	[105]
$Zr_{41.2}Ti_{13.8}Cu_{12.5}Ni_{10.0}Be_{22.5}$ (Vit 1)	Water quenching	DSC, SANS, TEM and APFIM	Zr-rich and Be-rich phases		[107–109]
$Zr_{28}Y_{28}Al_{22}Co_{22}$	Melt spinning	Dynamic Mechanical Analysis and TEM	$Y_{30.9}Zr_{26.0}Al_{24.8}Co_{18.3}$ and $Zr_{36.4}Y_{15.8}Al_{28.8}Co_{19.0}$	Phase separation observed during heating of a homogeneous glassy phase	[110]
$Zr_{60-x}Y_xAl_{15}Ni_{25}$ ($x = 15$, 27, and 45)	Melt spinning	DSC		Two supercooled liquid regions	[111]

a. Phase separation in solid state

- Pd-Si-Ag alloy / two amorphous phase formation after heating just above T_g

Chen and Turnbull, Acta Metall., 17, 1021 (1969)

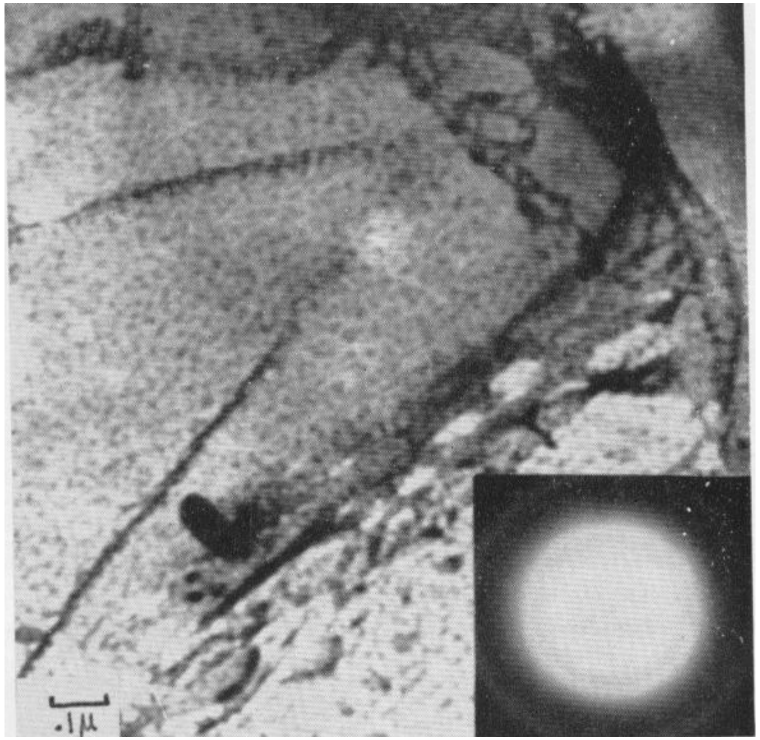

- After heating just above T_g, two amorphous separation occurs, but crystallization occurs simultaneously.

- Zr-Ti-Cu-Ni-Be BMG / small angle neutron scattering

Schneider et al, Appl. Phys. Lett., 68, 493 (1996)

decomposed during cooling in the liquid state to a two-phase mixture of Be-rich and Zr-rich glassy regions with a typical length scale of tens of nanometers

Martin et al., Acta Mater., 52, 4427 (2004)

Ti-rich and Be-depleted regions that appeared in the early stage of annealing due to the partitioning of alloying elements accompanied by the crystallization reaction.

* Zr-Y-Al-Ni system: homogeneous glassy phase in the as-quenched state had transformed into a mixed structure consisting of the Zr-rich Zr-Al-Ni glassy phase and the Y-rich Y-Al-Ni crystalline phase (3-5 nm).

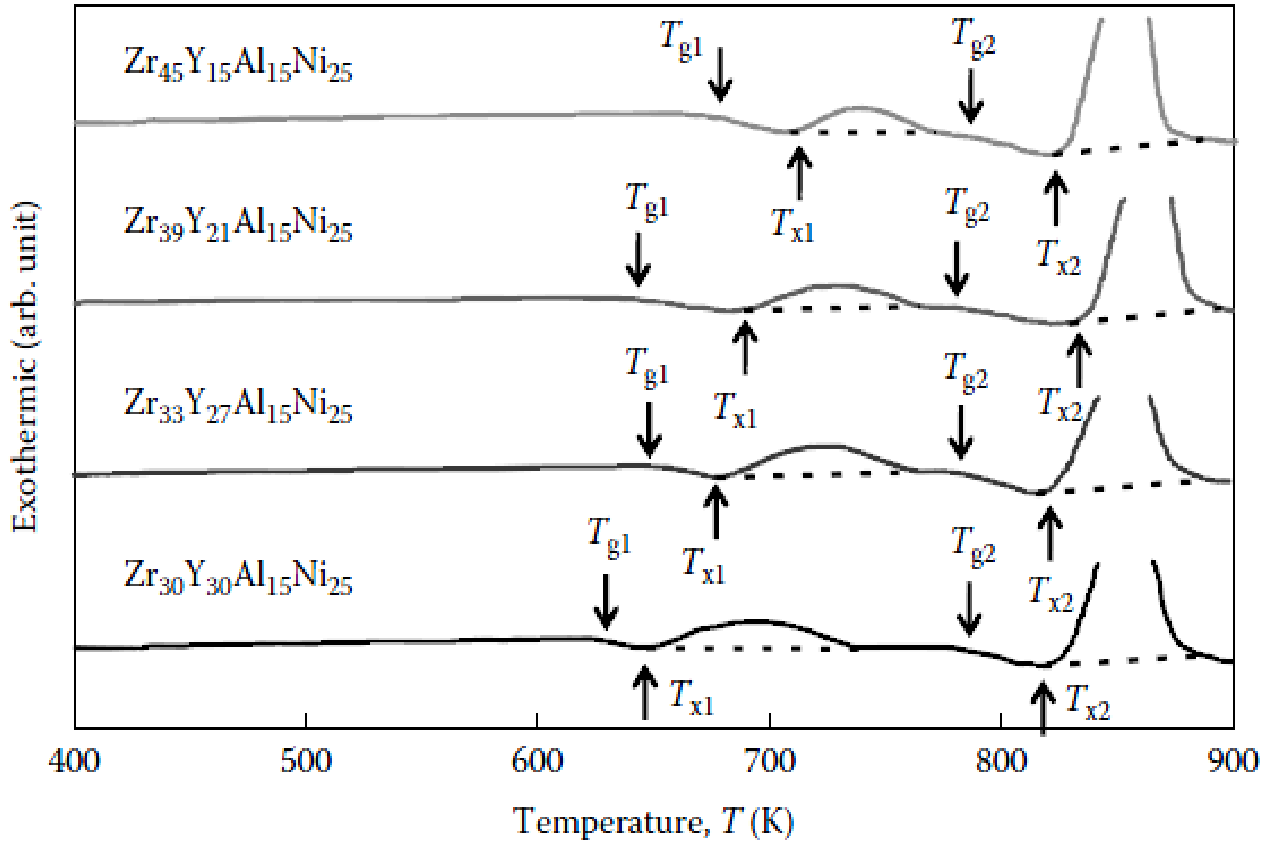

FIGURE 5.15
DSC curves of the glassy $Zr_{60-x}Y_xAl_{15}Ni_{25}$ ($x=15$, 21, 27 and 30) alloys obtained at a heating rate of 0.67 K s^{-1}(40 K min^{-1}). Note the presence of two T_gs and two T_xs in all the alloys studied. (Reprinted from Inoue, A. et al., *Mater. Sci. Eng. A*, 179/180, 346, 1994. With permission.)

* Zr-Y-Al-Ni system: exhibit two glass transition temperature

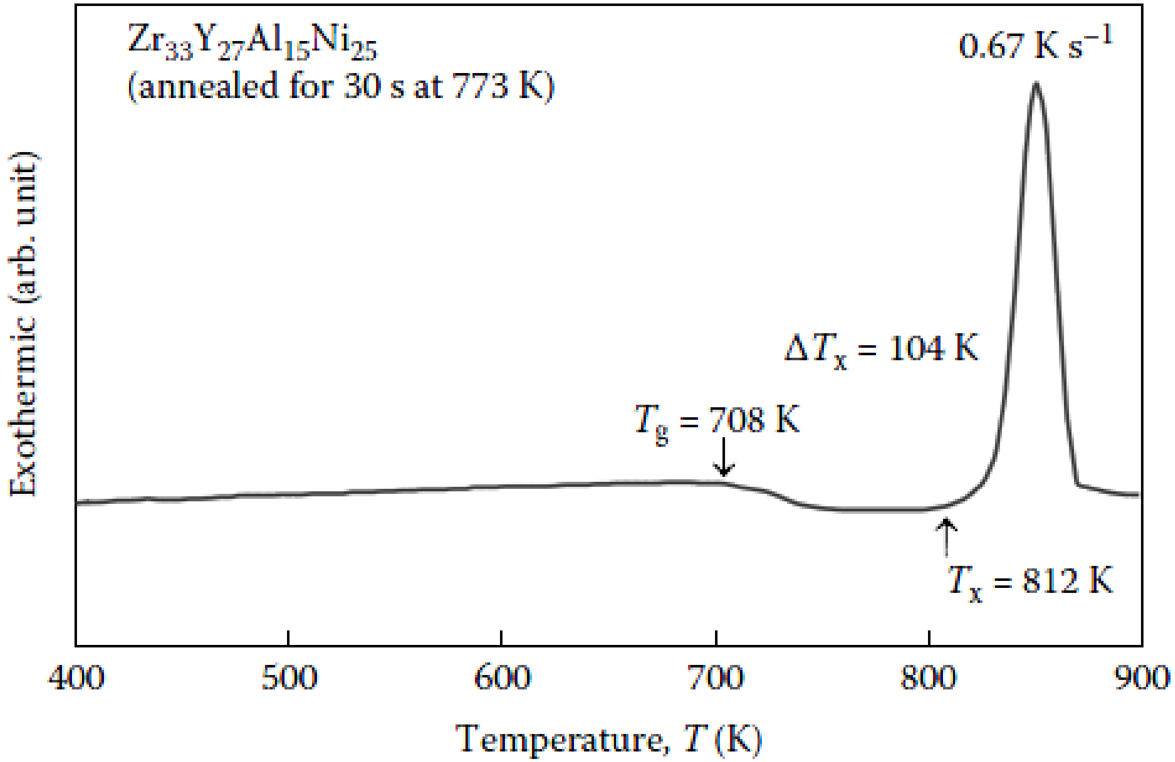

FIGURE 5.16
DSC curve of the glassy $Zr_{33}Y_{27}Al_{15}Ni_{25}$ alloy pre-annealed for 30 s at 773 K. The width of the supercooled liquid region, ΔT_x (= $T_x - T_g$), has now increased to 104 K from 40 K in the as-solidified condition. (Reprinted from Inoue, A. et al., *Mater. Sci. Eng. A*, 179/180, 346, 1994. With permission.)

b. Phase separation in liquid state

* La-Zr-Al-Cu-Ni system

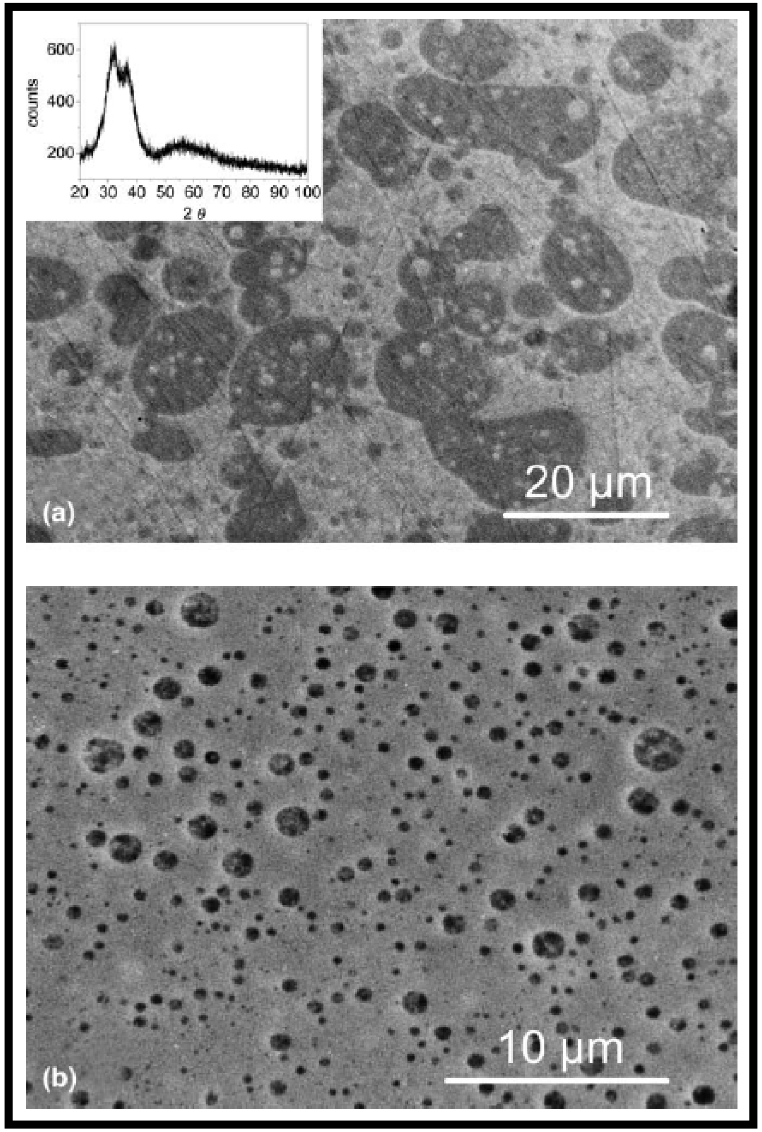

Kundig et al., *Acta Mat.*, 52 (2004) 2441-2448.

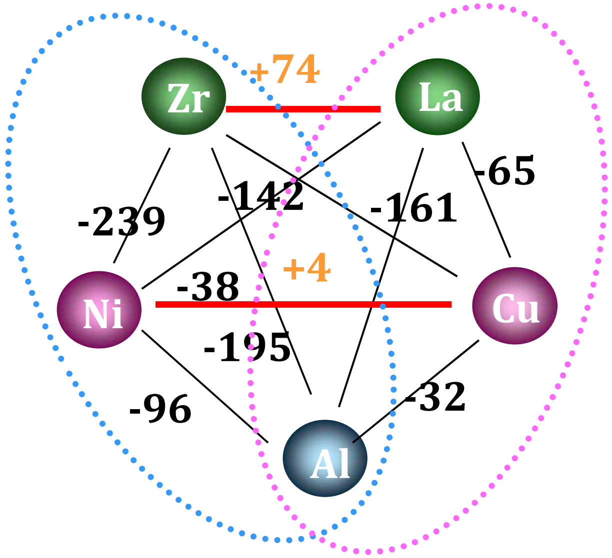

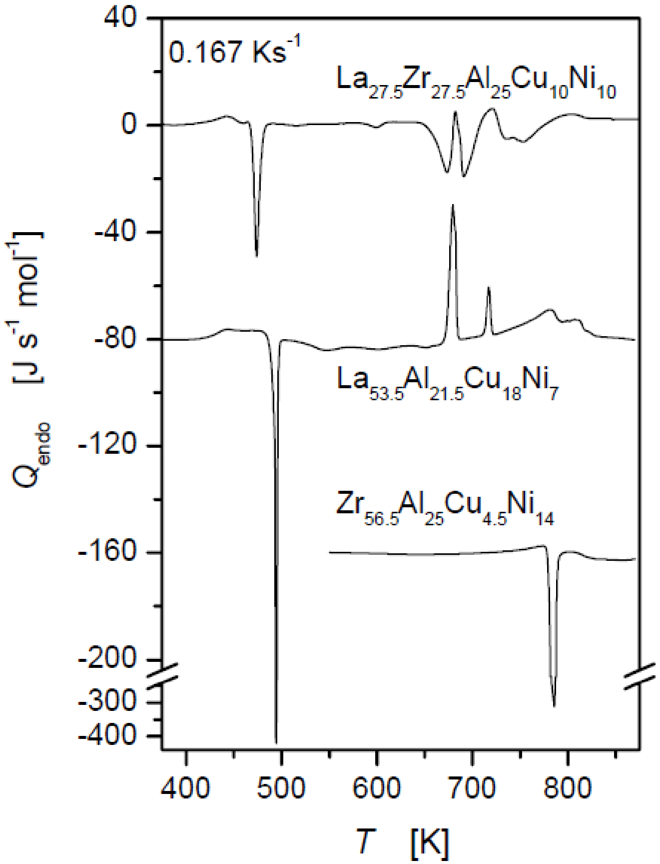

* La-Zr-Al-Cu-Ni system

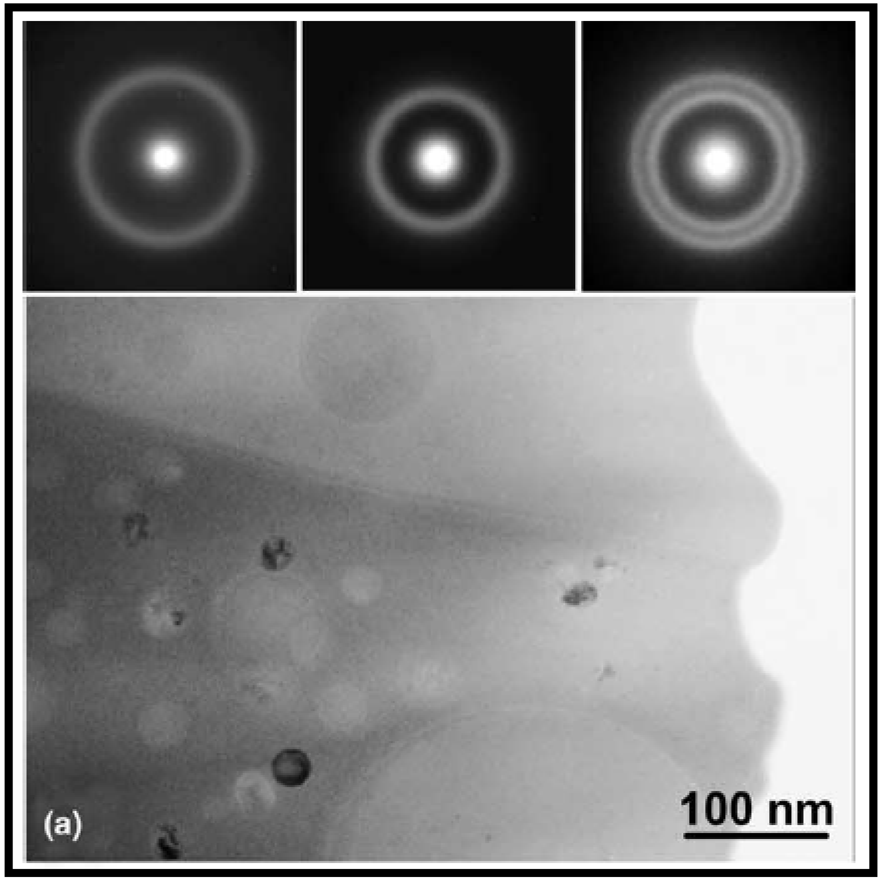

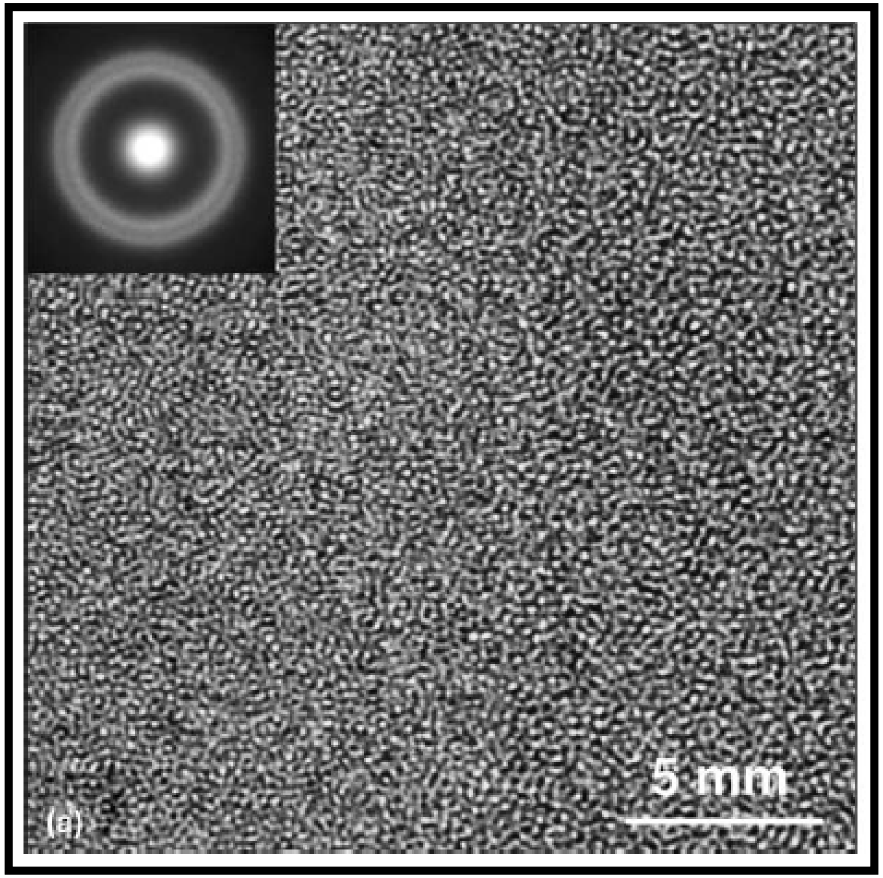

Kundig et al., *Acta Mat.*, 52 (2004) 2441-2448.

* La-Zr-Al-Cu-Ni system

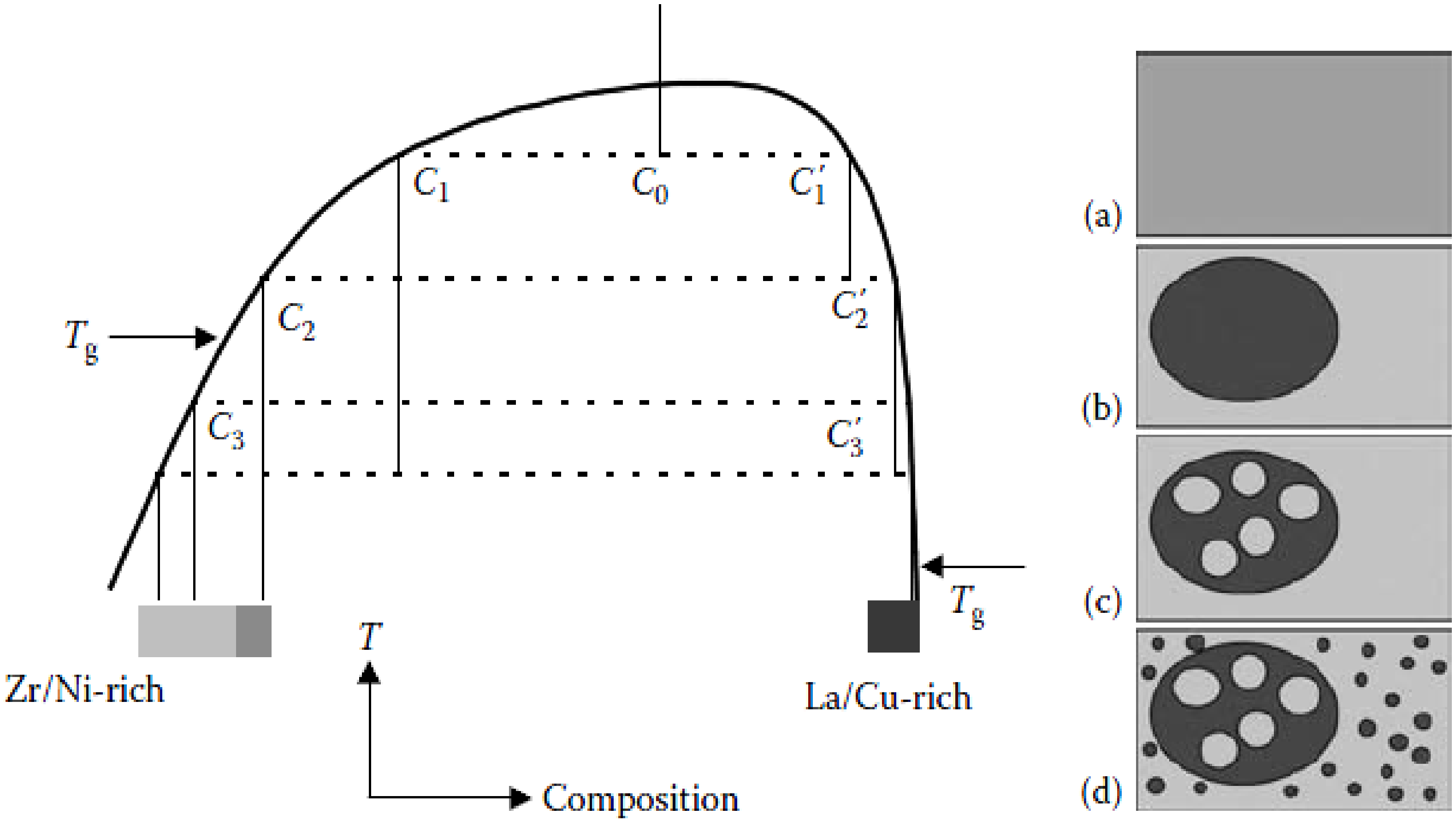

FIGURE 5.17
Schematic of the miscibility gap and the sequence of phase formation during cooling in the La–Zr–Al–Cu–Ni system. The positions of letters (a) to (d) in the diagram on the left correspond to the schematic microstructures (a) to (d) on the right. (Reprinted from Kündig, A.A. et al., *Acta Mater.*, 52, 2441, 2004. With permission.)

Shell/Yard region in phase separated structure

- Yard : Secondary phase-free region

  Shell : The layer enveloping primary phase by wetting

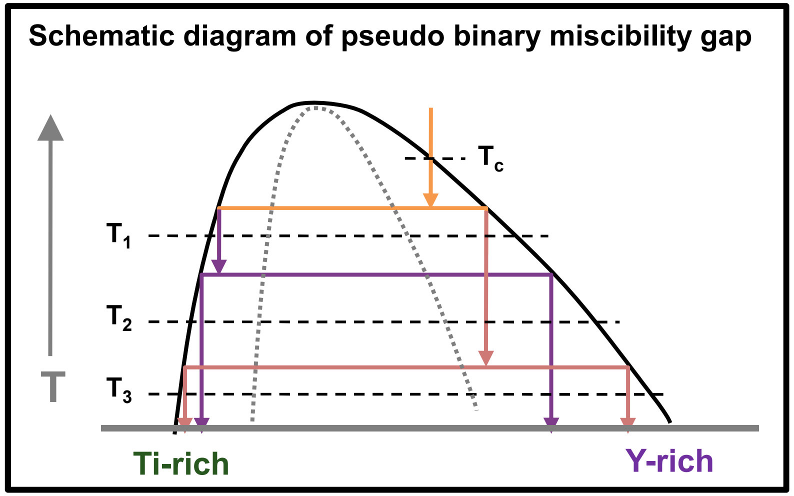

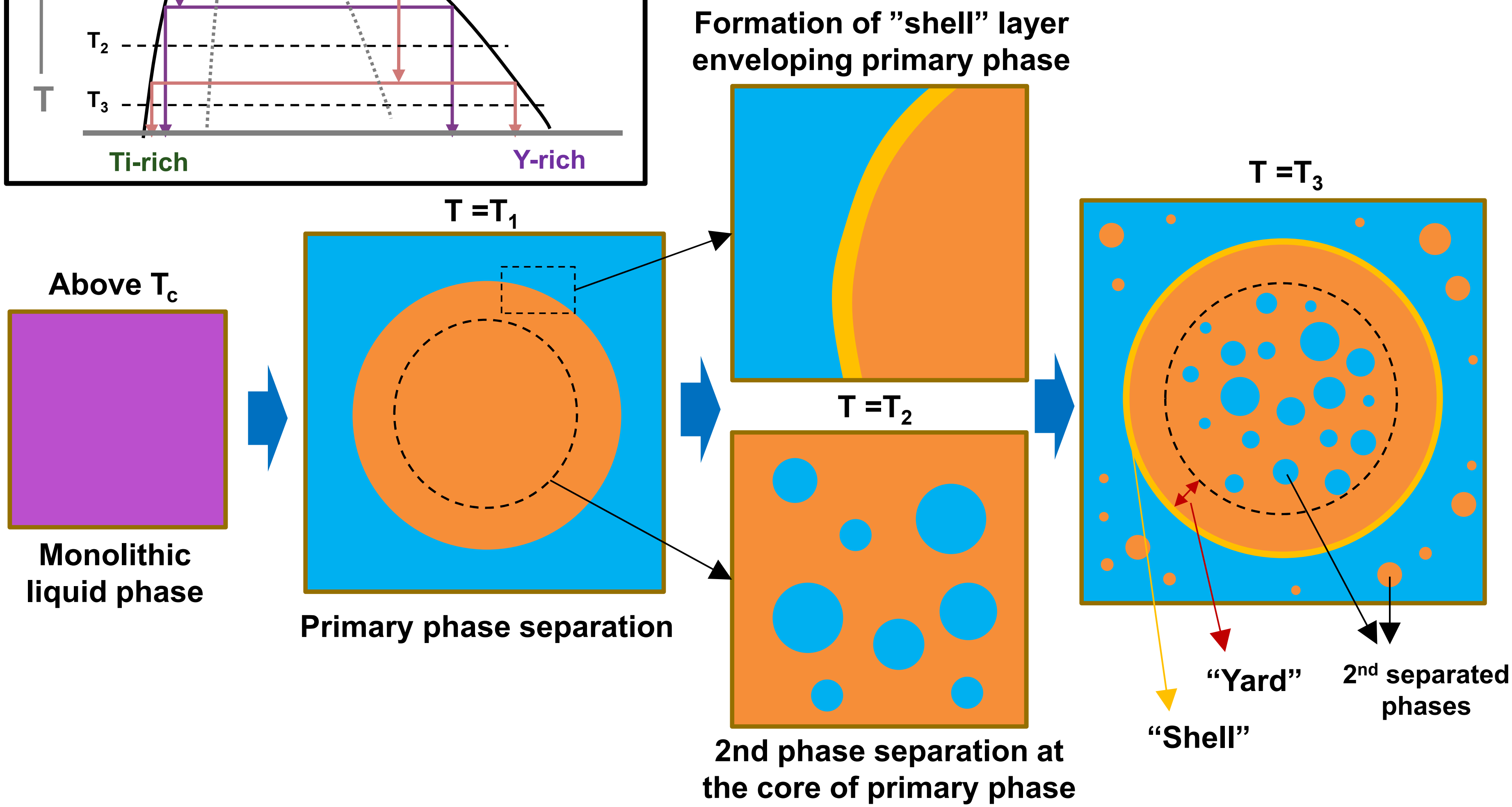

* Ti-Y-Al-Co system → $Ti_{24}Y_{18}La_{18}Al_{22}Co_{18}$ three different glassy phase

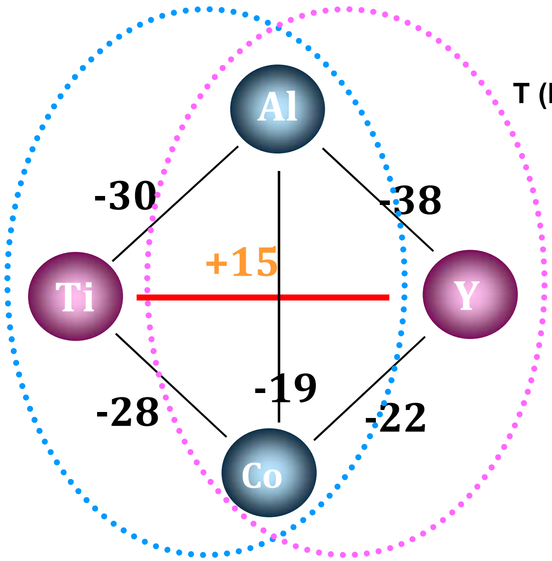

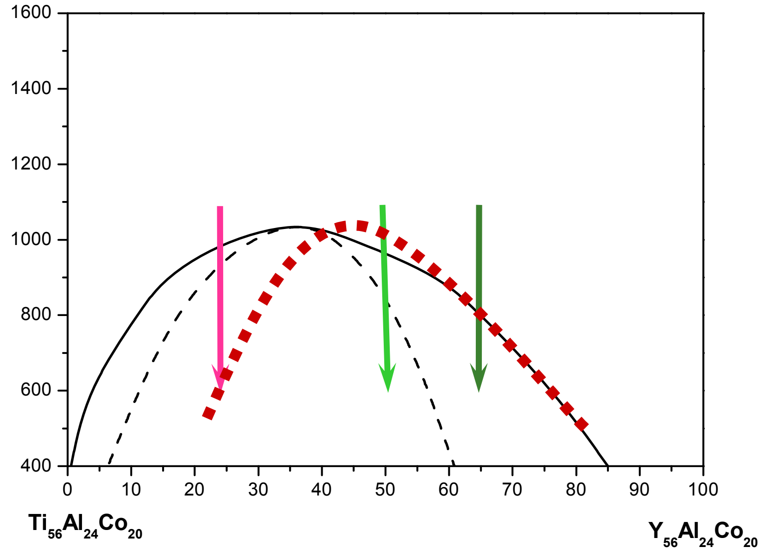

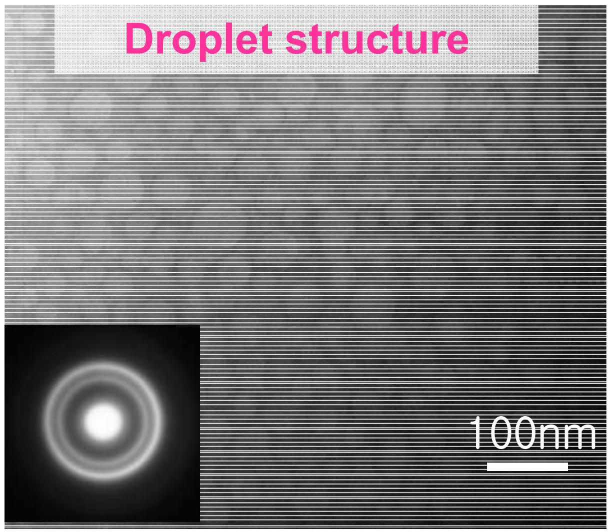

$(Y_{56}Al_{24}Co_{20})_{25}(Ti_{56}Al_{24}Co_{20})_{75}$

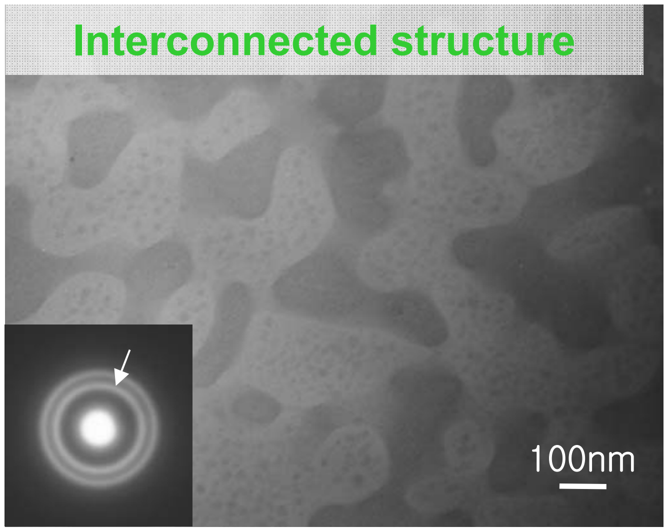

$(Y_{56}Al_{24}Co_{20})_{50}(Ti_{56}Al_{24}Co_{20})_{50}$

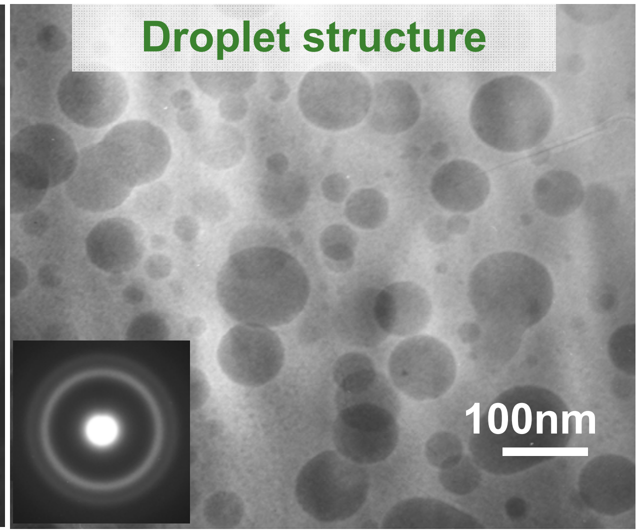

$(Y_{56}Al_{24}Co_{20})_{65}(Ti_{56}Al_{24}Co_{20})_{35}$

* Ti-Y-Al-Co system

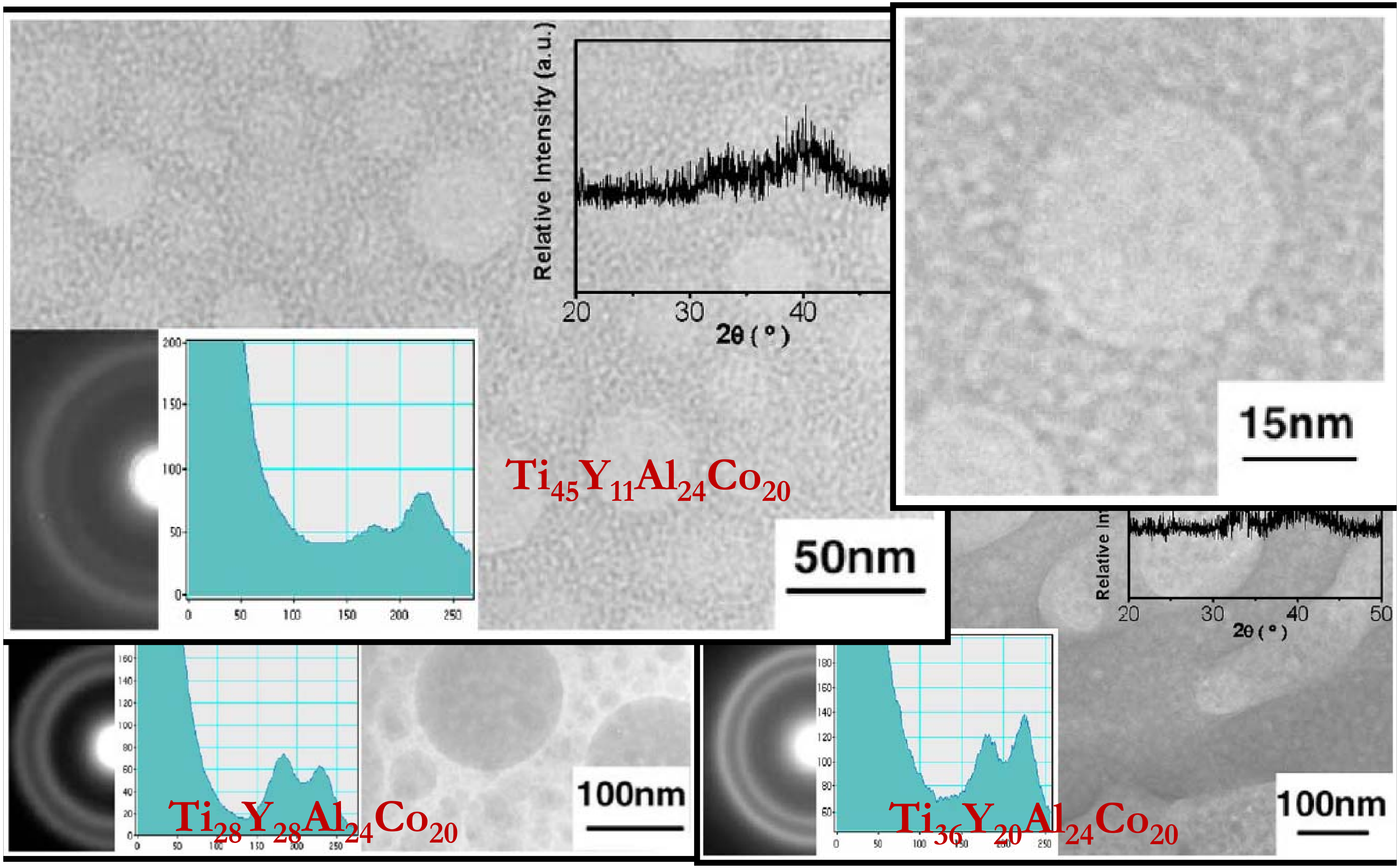

B.J.Park et al., *Appl. Phys. Lett.*. 85 (2004) 6353.
Phys. Rev. Lett., 96 (2006) 245503.

* Ni-Nb-Y system

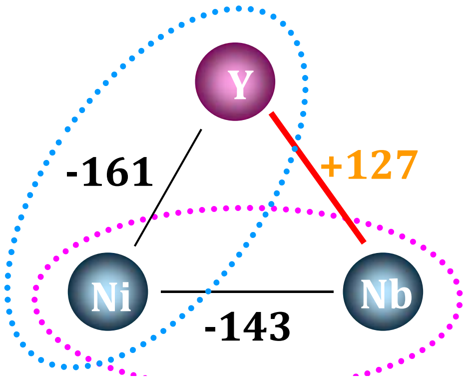

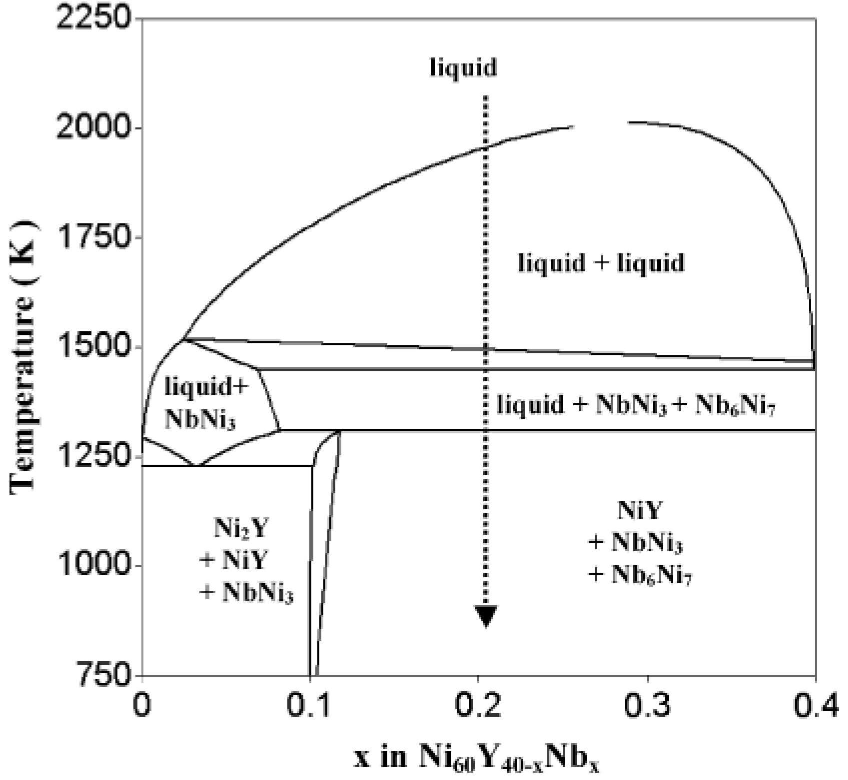

Fig. 4. Pseudo-binary section of the ternary phase diagram $Ni_{60}Y_{40}$–$Ni_{60}Nb_{40}$ calculated by CALPHAD method.

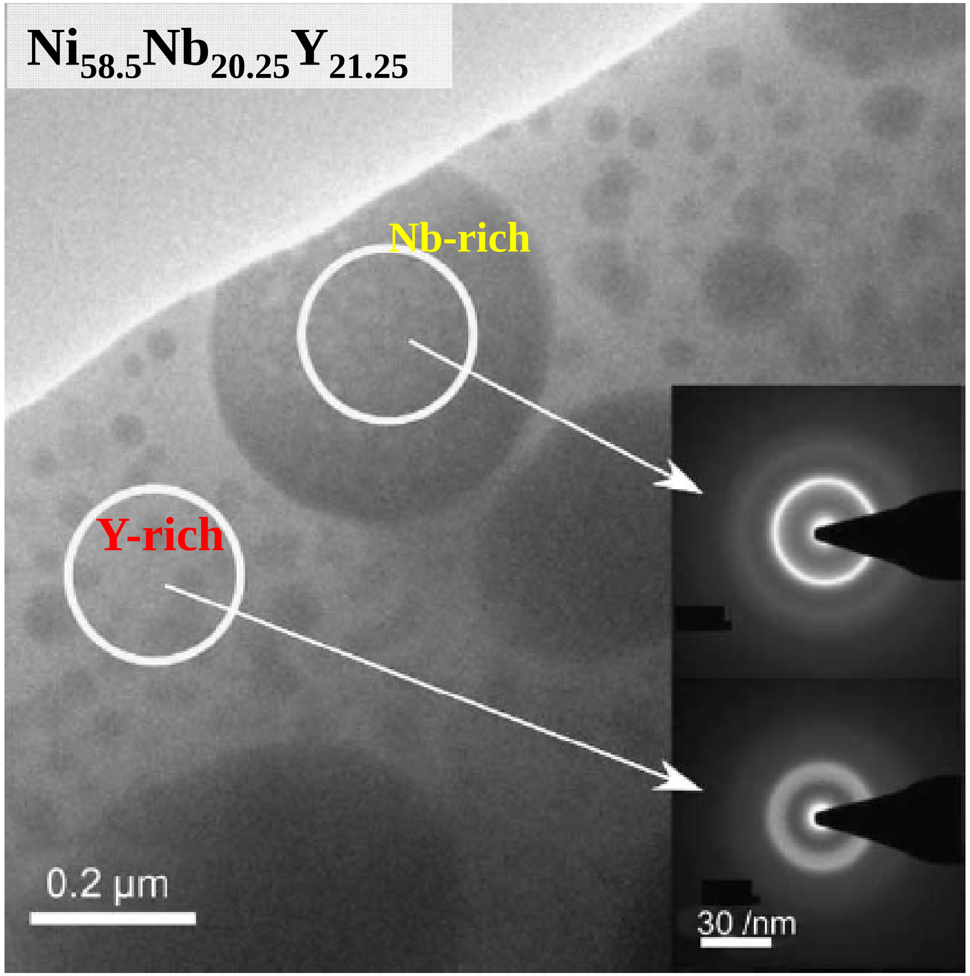

Mattern et al., *Scripta Mat.* 53 (2005) 271.
Mat. Sci. Eng. A, 449-451 (2007) 207.